

Table I. Luminescence and Transient Absorption Data for Octahedral Molybdenum(III) and Rhenium(IV) Complexes^a

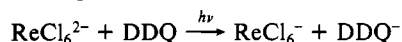
complex	λ_{exc}	λ_{em}	τ_{em}	λ_{abs}	τ_{abs}
Mo(NCS) ₆ ³⁻ ^b	355	1350	760	420	800
	835			425	760
	1279			475	760
MoCl ₆ ³⁻ ^c	532	1095	480	340	550
ReCl ₆ ²⁻ ^d	355	1330	130		
	620	1340	140	420	140

^a Abbreviations: exc = excitation, em = emission, abs = transient absorption. Wavelengths are given in nm and lifetimes ($\pm 10\%$) in ns. Excitation was via Nd:YAG laser (532, 355 nm) or Nd:YAG-pumped dye laser (620 nm, with H₂ Raman shifter to generate 835 and 1279 nm). ^b K₃Mo(NCS)₃·4H₂O in CH₃CN. ^c K₃MoCl₆ in 6 M HCl/saturated aqueous LiCl (1:1 v/v). ^d (Bu₄N)₂ReCl₆ in CH₃CN. The emission maximum is red-shifted slightly by self-absorption in the experiments involving 620-nm excitation, because they require substantially more concentrated solutions of (Bu₄N)₂ReCl₆.

Table I; Figures 2 and 3 show the absorption and emission spectra for MoCl₆³⁻ and ReCl₆²⁻ respectively. (The absorption spectrum of Mo(NCS)₆³⁻ in CH₃CN has been reported in ref 2.) The overlap of the absorption and emission spectra can be used to estimate the equilibrium energy of the lowest lying excited state in Mo(NCS)₆³⁻ (7700 cm⁻¹): to our knowledge, an experimental measurement of this energy has not been reported previously. (Excited-state energies obtained for MoCl₆³⁻ and ReCl₆²⁻ by this procedure, 9200 and 7600 cm⁻¹ respectively, are in agreement with the high-resolution spectroscopic results of Flint and co-workers.^{6,9}) The excitation spectra for these luminescences are very similar to the corresponding absorption spectra. With ReCl₆²⁻, for example, the excitation spectrum for luminescence at 1340 nm shows vibrational structure in the 600–750-nm ($\Gamma_8(^4A_{2g}) \rightarrow \Gamma_7, \Gamma_8(^2T_{2g})$) and 1000–1250-nm ($\Gamma_8(^4A_{2g}) \rightarrow \Gamma_8(^2T_{1g}), \Gamma_8(^2E_g)$) regions comparable to that observed in the absorption spectrum.

The low-lying doublet states in strong-field d³ complexes are ordinarily relatively long-lived because of the small changes in geometry that accompany the intraconfigurational transitions $\{^2T_{1g}, ^2E_g\} \rightarrow ^4A_{2g}$.⁴ Excited-state lifetimes well above 1 μ s have been observed for MoCl₆³⁻⁷ and ReCl₆²⁻^{8a} in the solid state. We have now also measured the lifetimes of the lowest excited states for all three complexes in solution, using both emission (τ_{em} ; see Table I) and transient absorption techniques (τ_{abs}).¹¹

Our previous study of Mo(NCS)₆³⁻² showed that the complex is capable of efficient excited-state redox reactions. The new data reported here represent direct measurements of the redox-active state of Mo(NCS)₆³⁻; comparable photophysical properties are now established for the other two ions as well. We have demonstrated by flash kinetic experiments,¹² for example, that photooxidation of ReCl₆²⁻ can be accomplished by 2,3-dichloro-5,6-dicyano-1,4-benzoquinone (DDQ):



The luminescence lifetimes for ReCl₆²⁻ and Mo(NCS)₆³⁻ are reduced in the presence of DDQ and 1,4-dinitrobenzene respectively.¹³ Thus, our results from flash irradiation of these two

complexes are now confirmed in separate luminescence measurements.

The experiments reported herein strongly suggest that a variety of second- and third-row d³ complexes will lend themselves readily to photophysical as well as photochemical study. Several aspects of these new photochemical systems are currently under investigation: We are examining the possibility of a spontaneous second electron transfers following initial photoredox processes in ReCl₆²⁻ and MoCl₆³⁻. Also, both our previous study of Mo(NCS)₆³⁻² and flash-photolysis experiments now in progress with other acceptors and ReCl₆²⁻¹² suggest that upper excited states may be sufficiently long-lived in these solutions to undergo independent bimolecular redox reactions.

Acknowledgment. We thank Professor Dewey Holten for helpful discussions and Dr. Xinwei Yan for assistance with the nanosecond laser measurements. This research was supported by the National Science Foundation (Grant CHE-8601008, to A. W.M.; Grant CHE-8306587, for the nanosecond laser apparatus).

Registry No. Mo(NCS)₆³⁻, 35215-16-8; MoCl₆³⁻, 15203-34-6; ReCl₆²⁻, 16871-50-4.

Department of Chemistry
Washington University
St. Louis, Missouri 63130

Qin Yao

Department of Chemistry
Louisiana State University
Baton Rouge, Louisiana 70803-1804

Andrew W. Maverick*

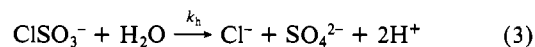
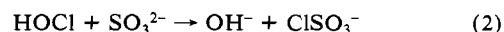
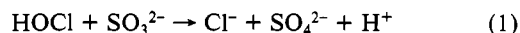
Received November 23, 1987

Kinetics of Hydrolysis of the Chlorosulfate Ion

Sir:

Chlorosulfuric acid (ClSO₃H) is a very strong acid that reacts explosively when mixed with water.¹ This has prevented use of chlorosulfuric acid to measure the rate of hydrolysis of the chlorosulfate ion. Recent studies by the pulsed-accelerated-flow method^{2,3} show that the reaction between HOCl and SO₃²⁻ is extremely rapid (1.6 × 10⁹ M⁻¹ s⁻¹ at 25.0 °C).⁴ This is 5 orders of magnitude faster than the reaction between OCl⁻ and SO₃²⁻.⁵ Although the latter reaction has been postulated to occur by oxygen atom transfer,⁵ earlier attempts to measure ¹⁸O exchange between sulfite and hypochlorous acid gave inconclusive results.⁶ The magnitude of the HOCl rate constant and the evidence for Cl⁺ transfer in the acid-assisted reactions⁷ of NH₂Cl with SO₃²⁻ lead to the proposal that ClSO₃⁻ is an intermediate for the HOCl reaction as well.⁴ The Cl⁺-transfer reaction corresponds to a nucleophilic attack by the sulfur of SO₃²⁻ on the chlorine of HOCl to eliminate OH⁻.

Direct oxygen atom transfer (eq 1) would give immediate release of acid, whereas Cl⁺ transfer will first release base (eq 2) and the subsequent hydrolysis of chlorosulfate will then release acid (eq 3). This study uses indicator reactions, which are



(10) The photomultiplier detector from a Spex Fluorolog 2 Model F112X instrument was replaced with a Ge photovoltaic detector (77 K; Judson J16-D, 2 mm diameter); the emission spectral bandwidth in Figures 2 and 3 was ca. 10 nm. For phosphorescence lifetime measurements, the same detector was used with a Quantel Datachrom 5000 Nd:YAG laser, except that the detector was operated at room temperature (response time <100 ns). Comparison of our lifetimes in solution with those for solids containing MoCl₆³⁻⁷ and ReCl₆²⁻ suggests that phosphorescence quantum yields are <10⁻³ in all of our experiments.

(11) Deviations in the order of observed luminescence lifetimes from that expected on the basis of the energy-gap law (see, for example: Caspar, J. V.; Meyer, T. J. *Inorg. Chem.* **1983**, *22*, 2444–2453) may be due to differences in solvents and accessible vibrational modes and in the nature of the lowest energy excited states among the three complexes.

(12) Lord, M. D.; Henderson, L. J., Jr.; Maverick, A. W., unpublished work.

(13) The lifetime quenching can only be measured qualitatively with the present apparatus, because both luminescence signals are relatively weak and, in the case of ReCl₆²⁻, because the measured lifetime is close to the response time of the Ge detector.

(1) Cotton, F. A.; Wilkinson, G. *Advanced Inorganic Chemistry*, 4th ed.; Wiley: New York, 1980; p 540.

(2) Nemeth, M. T.; Fogelman, K. D.; Ridley, T. Y.; Margerum, D. W. *Anal. Chem.* **1987**, *59*, 283–291.

(3) Jacobs, S. A.; Nemeth, M. T.; Kramer, G. W.; Ridley, T. Y.; Margerum, D. W. *Anal. Chem.* **1984**, *56*, 1058–1065.

(4) Fogelman, K. D.; Walker, D. M.; Margerum, D. W., to be submitted for publication.

(5) Lister, M. W.; Rosenblum, P. *Can. J. Chem.* **1963**, *41*, 3013–3020.

(6) Halperin, J.; Taube, H. *J. Am. Chem. Soc.* **1952**, *74*, 375–380.

(7) Yiin, B. S.; Walker, D. M.; Margerum, D. W. *Inorg. Chem.* **1987**, *26*, 3435–3441.

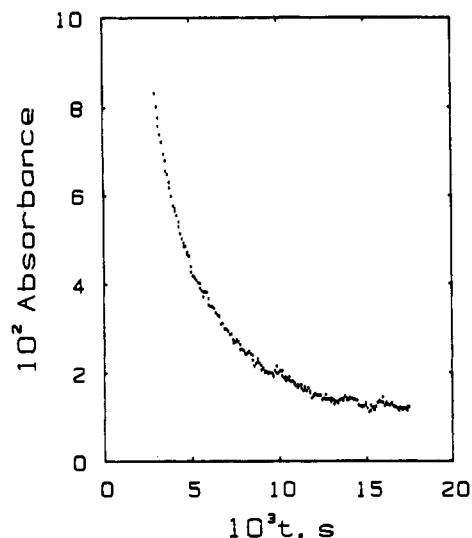


Figure 1. Indicator (2,4-dinitrophenol) observation of the hydrolysis of ClSO_3^- measured with the Durrum stopped-flow instrument (conditions in Table I).

Table I. First-Order Rate Constants for the Hydrolysis of the Chlorosulfate Ion^a

temp, K	k_h, s^{-1}	temp, K	k_h, s^{-1}
275.0	48 ± 2	293.0	211 ± 13
278.0	63 ± 5	298.0	294 ± 44
283.0	92 ± 5	298.0	254 ± 8^b
288.0	124 ± 4	298.0	258 ± 9^b

^a Conditions: ionic strength = $(8 \pm 2) \times 10^{-4}$; Hi-Tech stopped-flow with 2-mm path, 410 nm; $[\text{HOCl}] = [\text{SO}_3\text{H}^-] = 2.57 \times 10^{-4}$ M; initial pH = 4.00 ± 0.03 ; [2,4-dinitrophenol] = 1.18×10^{-5} M; k_h values are corrected for mixing effects, $k_{\text{mix}} = 1000 \text{ s}^{-1}$. ^b Durrum stopped-flow instrument with 1.88-cm path; k_h values are corrected for mixing effects, $k_{\text{mix}} = 1700 \text{ s}^{-1}$.

followed by stopped-flow methods, to prove that reactions 2 and 3 take place rather than reaction 1. This method allows the first measurement of the kinetics of chlorosulfate hydrolysis.

When NaOCl (5.00×10^{-4} M) and Na_2SO_3 (5.08×10^{-4} M) solutions, both adjusted to pH 8, are mixed in the presence of phenolphthalein ($\text{p}K_a = 9.55$),⁸ the solution immediately turns pink and then fades to colorless. Similar evidence for rapid release of OH^- followed by measurable release of H^+ is found for reactions in the presence of thymol blue ($\text{p}K_a = 9.20$).⁹ The indicator 2,4-dinitrophenol ($\text{p}K_a = 4.11$)⁹ was selected to measure the k_h rate constant for ClSO_3^- hydrolysis by stopped-flow spectroscopy at 410 nm. Figure 1 shows the result of mixing equal volumes of 5.14×10^{-4} M HOCl (pH 4.01) and 5.14×10^{-4} M NaHSO_3 (pH 3.97 with 2.35×10^{-5} M indicator). The formation of ClSO_3^- is extremely rapid, and its hydrolysis causes a measurable decrease of the yellow color with the release of acid (eq 3). The final pH is 3.46 (25.0 °C), so that interference from HSO_4^- ($\text{p}K_a = 1.85$) is minimal. (The indicator decomposes slowly in the presence of HOCl , so it is added to the NaHSO_3 solution before mixing.¹⁰)

It can be shown that the absorbance values (A_0 , initial; A_∞ , final; A_t , a function of time) fit eq 4 for first-order kinetics of hydrolysis

$$\ln \left[\frac{1/A_t - 1/A_\infty}{1/A_0 - 1/A_\infty} \right] = -k_h t \quad (4)$$

of ClSO_3^- . Reactions were measured from 2.0 to 25.0 °C (Table I) with a Hi-Tech Scientific stopped-flow system.¹¹ A 2-mm

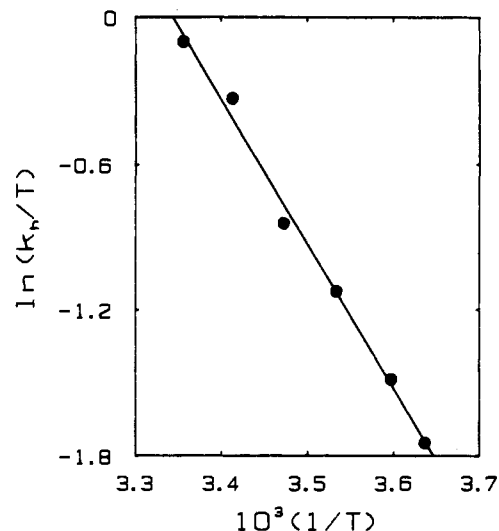


Figure 2. Eyring plot for the temperature dependence of k_h , where $\Delta H^\ddagger = 49 \text{ kJ mol}^{-1}$ and $\Delta S^\ddagger = -32 \text{ J mol}^{-1} \text{ K}^{-1}$.

observation path was used, and data were corrected for mixing effects,¹² $k_h = k_{\text{obsd}}/(1 - k_{\text{obsd}}/k_{\text{mix}})$ where $k_{\text{mix}} = 1000 \text{ s}^{-1}$ for this instrument. Five or more runs were measured at each temperature. The 25.0 °C rate constants were also measured in two sets of experiments with a Durrum stopped-flow system where k_{mix} is 1700 s^{-1} .¹² The average k_h value for three sets of data at 25.0 °C is $(2.7 \pm 0.2) \times 10^2 \text{ s}^{-1}$. A plot of $\ln(k_h/T)$ against $1/T$ (Figure 2) gives $\Delta H^\ddagger = 49 \pm 2 \text{ kJ mol}^{-1}$ and $\Delta S^\ddagger = -32 \pm 1 \text{ J mol}^{-1} \text{ K}^{-1}$. Estimated k_h values obtained with other indicators at higher pH indicate that the hydrolysis rate constant is not affected by the acidity of the solution from pH 3.5 to 9.

The negative activation entropy for the ClSO_3^- hydrolysis corresponds to the uptake of one water molecule ($-29 \text{ J mol}^{-1} \text{ K}^{-1}$) from aqueous solution.¹³ This indicates that the composition of the transition state is $[\text{H}_2\text{OSO}_3\text{Cl}]^\ddagger$, where sulfur is five-coordinate.

The k_h value for ClSO_3^- at 25.0 °C is a factor of 1.3×10^9 larger than the hydrolysis rate constant for FSO_3^- . Fluorosulfate hydrolysis is both acid and base catalyzed, but the reaction with H_2O ($k_h = 2.1 \times 10^{-7} \text{ s}^{-1}$) is the dominant path between pH 3 and 12.¹⁴ The ΔS^\ddagger values for FSO_3^- hydrolysis are also negative, $-125 \text{ J mol}^{-1} \text{ K}^{-1}$ for the H_2O path and $-88 \text{ J mol}^{-1} \text{ K}^{-1}$ for the OH^- path.¹⁵

Our preliminary study of the hydrolysis of iodosulfate ion (formed from the reaction of I_2 and SO_3^{2-}) gives a k_h value (25.0 °C, $\mu = 0.005\text{--}0.015$) of $294 \pm 7 \text{ s}^{-1}$ in the pH range 3.3–7.8. This rate constant for ISO_3^- is in fair agreement with a value of 130 s^{-1} at 17 °C that was estimated from the temperature increase observed in continuous-flow mixing of I_2 and Na_2SO_3 solutions.¹⁶

Recent work in our laboratory shows that a number of non-metal redox reactions occur via Cl^\ddagger -transfer mechanisms (i.e. nucleophilic attack at chlorine). This includes acid-assisted reactions of NH_2Cl and OCl^- with I^- , Br^- , and SO_3^{2-} , where ICl , BrCl , and ClSO_3^- intermediates are postulated.^{7,17,18} The present study confirms that nucleophilic attack by SO_3^{2-} on HOCl (eq 2) is much more favorable at chlorine than at oxygen. Hydroxide ion is a reasonable leaving group in aqueous solutions. The subsequent rate of hydrolysis of ClSO_3^- is rapid, but is not in-

(8) Kolthoff, I. M. *Acid-Base Indicators*; Macmillan: New York, 1937; p 222.

(9) Kolthoff, I. M. *J. Phys. Chem.* **1930**, *34*, 1466–1483.

(10) Seyewetz, A.; Chaix, E. *Bull. Soc. Chim. Fr. Mem.* **1927**, *41*, 196–205.

(11) Wang, Y. L.; Lee, H. D.; Beach, M. W.; Margerum, D. W. *Inorg. Chem.* **1987**, *26*, 2444–2449.

(12) Dickson, P. N.; Margerum, D. W. *Anal. Chem.* **1986**, *58*, 3153–3158.

(13) (a) Koval, C. A.; Margerum, D. W. *Inorg. Chem.* **1981**, *20*, 2311–2318.

(b) Youngblood, M. P.; Margerum, D. W. *Inorg. Chem.* **1980**, *19*, 3068–3072.

(14) Jones, M. M.; Lockhart, W. L. *J. Inorg. Nucl. Chem.* **1968**, *30*, 1237–1243.

(15) Ryss, I. G.; Drabkina, A. Kh. *Kinet. Katal.* **1966**, *7*(2), 319–322.

(16) Inoue, H.; Sudo, Y. *Kogyo Kagaku Zasshi* **1967**, *70*, 123–126.

(17) Kumar, K.; Day, R. A.; Margerum, D. W. *Inorg. Chem.* **1986**, *25*, 4344–4350.

(18) Kumar, K.; Margerum, D. W. *Inorg. Chem.* **1987**, *26*, 2706–2711.

stantaneous. The activation parameters indicate the addition of water before the loss of Cl^- in the hydrolysis of ClSO_3^- .

Above pH 12.5 the reaction between OCl^- and SO_3^{2-} does not have a pH dependence.⁴ The indicator method is not suitable at high pH, and the rate of this reaction (followed by the disappearance of OCl^-) is no longer rapid compared to the rate of hydrolysis of ClSO_3^- at lower pH. Although, it is also possible for water to act as a general acid to assist a Cl^+ -transfer mechanism, we cannot rule out an oxygen atom transfer path above pH 12.5.

Acknowledgment. This work was supported by National Science Foundation Grants CHE-8616666 and CHE-8720318.

Registry No. HOCl , 7790-92-3; SO_3^{2-} , 14265-45-3; ClSO_3^- , 15181-48-3.

Department of Chemistry
Purdue University
West Lafayette, Indiana 47907

Boudin S. Yiin
Dale W. Margerum*

Received December 18, 1987

Synthesis and Characterization of the Luminescent Dithiolate-Bridged Dimer $[\eta\text{-Bu}_4\text{N}]_2[\text{Au}(i\text{-MNT})]_2$ ($i\text{-MNT} = \text{S}_2\text{C}_2(\text{CN})_2$) and Its Structurally Characterized, Metal-Metal-Bonded Gold(II) Oxidation Product $[\text{Ph}_4\text{As}]_2[\text{Au}(i\text{-MNT})\text{Cl}]_2$

Sir:

Although Burmeister et al.¹ suggested nearly 10 years ago that Au^{I} -dichlorocarbamate dimers are oxidized by halogens and pseudohalogen to metal-metal-bonded Au^{II} species, oxidized products could not be characterized structurally due to disproportionation into $[\text{Au}^{\text{III}}(\text{dte})_2]\text{Au}^{\text{I}}\text{X}_2$ ($\text{X} = \text{halide, pseudohalide}$).¹ Proton NMR data for the di-*n*-butyldithiocarbamate derivative $[\text{Au}(\text{dte})(\text{SCN})]_2$, however, was entirely consistent with the metal-metal-bonded formulation. Since this complex appears to be the only metal-metal-bonded Au^{II} dimer not containing Au-C bonds and since the Au^{I} dimer $[\text{Au}^{\text{I}}(\text{dte})]_2$ has a very short (2.78 Å) Au-Au distance,^{2,3} we embarked upon the synthesis and structural characterization of Au^{I} and Au^{II} dimers with sulfur-bonded ligands.

The Au^{I} dimer⁴ $\text{Au}_2(\text{MTP})_2$ ($\text{MTP} = \text{CH}_2\text{P}(\text{S})\text{Ph}_2$) has a normal (3.0 Å) $\text{Au}^{\text{I}}\cdots\text{Au}^{\text{I}}$ separation and is oxidized by halogens to both homovalent $\text{Au}^{\text{II}}\text{-Au}^{\text{II}}$ and heterovalent $\text{Au}^{\text{III}}\cdots\text{Au}^{\text{I}}$ species.^{5a} The stability of the Au^{II} MTP dimers $[\text{Au}(\text{MTP})\text{X}]_2$ ($\text{X} = \text{halides}$) suggested that by using electron-donating sulfur ligands stronger than dithiocarbamates it might be possible to isolate and characterize Au^{II} dimers with sulfur atom bridging ligands. The *i*-MNT ligand and other analogues formed from CS_2 proved to be suitable choices. Here we report the first structural characterization of a nonorganometallic Au^{II} metal-metal-bonded dimer containing one of the shortest Au-Au distances known (2.55 Å), the structure of the Au^{I} precursor, which also has a short (2.79 Å) Au-Au distance, and a preliminary description of the luminescent properties of this Au^{I} product.

Compound $\text{K}_2[\text{Au}^{\text{I}}(i\text{-MNT})]_2$ (**1a**) was obtained quantitatively from the reaction of⁶ $[\text{Au}(\text{PPh}_3)]_2(i\text{-MNT})$ with 1 molar equiv

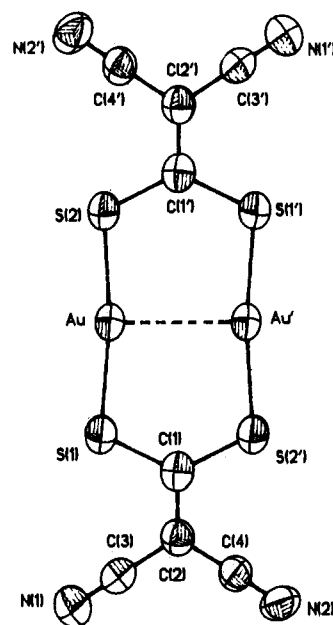


Figure 1. Structure of $[\eta\text{-Bu}_4\text{N}]_2[\text{Au}(i\text{-MNT})]_2$ (**1b**). Bond lengths (Å): Au-Au', 2.796 (1); Au-S(1), 2.283 (2); Au-S(2), 2.280 (2); S(1)-C(1), 1.735 (9); S(2)-C(1), 1.727 (8); C(1)-C(2), 1.37 (1); C(2)-C(3), 1.46 (1); C(2)-C(4), 1.43 (1); C(3)-N(1), 1.13 (1); C(4)-N(2), 1.15 (1). Bond angles (deg): S(1)-Au-S(2), 172.2 (1); S(1)-C(1)-S(2)', 127.5 (4); C(1)-C(2)-C(3), 122.9 (8); C(1)-C(2)-C(4), 123.1 (7); C(2)-C(3)-N(1), 178 (1); C(2)-C(4)-N(2), 177.8 (9); C(3)-C(2)-C(4), 114.1 (7).

of $\text{K}_2(i\text{-MNT})$ in CH_2Cl_2 at 22 °C. Addition of $[\eta\text{-Bu}_4\text{N}]\text{Br}$ or $[\text{Ph}_4\text{As}]\text{Cl}$ to the CH_2Cl_2 solution of **1a** resulted in the formation of $[\eta\text{-Bu}_4\text{N}]_2[\text{Au}(i\text{-MNT})]_2$ (**1b**) in 80% yield and $[\text{Ph}_4\text{As}]_2[\text{Au}(i\text{-MNT})]_2$ (**1c**) in 85% yield, respectively. Compound **1b** was characterized by IR spectroscopy and elemental⁷ and single-crystal X-ray diffraction analyses.⁸

The molecular structure and important bond distances and angles of **1b** are given in Figure 1. The two gold atoms are bridged by two *i*-MNT ligands by bonding through the sulfur atoms: Au-S(1) = 2.283 (2) Å; Au-S(2) = 2.280 (2) Å. The coordination of the sulfur atoms to the Au^{I} center is linear: S(1)-Au-S(2)' = 172.2 (1)°. The anion is nearly planar. The most interesting feature in this molecule is the unusually short Au-Au distance, 2.796 (1) Å, significantly shorter than the distance observed in metallic gold (2.884 Å)⁹ and similar to the short Au-Au distances observed in dialkyldithiocarbamate-bridged Au^{I} dimers (2.76-2.79 Å).^{2,3}

The compound $[\text{Au}(\text{PPh}_3)]_2(i\text{-MNT})$ displays a strong visible luminescence at 77 K in CH_3CN solution with two emission components at ~525 nm having 33 and 286 μs lifetimes (355-nm

- Calabro, D. C.; Harrison, B. A.; Palmer, G. T.; Moguel, M. K.; Rebbert, R. L.; Burmeister, J. L. *Inorg. Chem.* **1981**, *20*, 4311.
- (a) Hesse, R.; Jennische, P. *Acta Chem. Scand.* **1972**, *26*, 3855. (b) Jennische, P.; Anacker-Eickhoff, H.; Wahlberg, A. *Acta Crystallogr., Sect. A: Cryst. Phys., Diffraction, Theor. Gen. Crystallogr.* **1975**, *A31*, S143.
- Farrell, F. J.; Spiro, T. G. *Inorg. Chem.* **1971**, *10*, 1606.
- Mazany, A. M.; Fackler, Jr., J. P. *J. Am. Chem. Soc.* **1984**, *106*, 801.
- (a) Basil, J. D.; Murray, H. H.; Fackler, Jr., J. P.; Tocher, J.; Mazany, A. M.; Trzcinska-Bancroft, B.; Knachel, H.; Dudis, D.; Delord, T. J.; Marler, D. O. *J. Am. Chem. Soc.* **1985**, *107*, 6908 and references therein. (b) Schmidbaur, H.; Franke, R. *Inorg. Chim. Acta* **1975**, *13*, 79.
- Khan, M. N. I.; Wang, S.; Heinrich, D. D.; Fackler, Jr., J. P. *Acta Crystallogr.*, in press.

- IR (KBr, Nujol, ν_{CN}): **1b**, 2190 (s), 2200 (sh) cm^{-1} ; **2b**, 2200 (s) cm^{-1} . Anal. Calcd for **1b**: C, 41.45; H, 6.22; N, 7.25. Found: C, 41.72; H, 6.03; N, 7.15. Calcd for **2b**: C, 52.71; H, 3.29; N, 4.61. Found: C, 52.52; H, 3.21; N, 4.56.
- Crystal data. **1b**: $\text{C}_{40}\text{H}_{72}\text{Au}_2\text{S}_4\text{N}_6$, $M_r = 1157.4$, monoclinic, space group, $P2_1/c$, $a = 14.228$ (3) Å, $b = 8.754$ (2) Å, $c = 20.360$ (3) Å, $\beta = 107.49$ (1)°, $V = 2418.5$ (8) Å³, $Z = 2$, $D_{\text{calcd}} = 1.59$ g cm^{-3} . **2b**: $\text{C}_{56}\text{H}_{40}\text{Au}_2\text{As}_2\text{Cl}_2\text{N}_4\text{S}_4$, $M_r = 1510.8$, triclinic, space group, $P\bar{1}$, $a = 11.619$ (2) Å, $b = 12.404$ (5) Å, $c = 11.108$ (2) Å, $\alpha = 98.20$ (3)°, $\beta = 105.70$ (2)°, $\gamma = 110.54$ (2)°, $V = 1372.3$ (7) Å³, $Z = 1$, $D_{\text{calcd}} = 1.80$ g cm^{-3} . Data were collected on a Nicolet R3m/E diffractometer. Structure solution and refinements were carried out by using the SHELXTL collection of crystallographic software. The structures of **1b** and **2b** were solved by heavy-atom methods. Convergence to final R values of $R = 0.0292$ and $R_w = 0.0304$ for **1b** was obtained by using 2291 reflections [$F^2 \geq 3\sigma(F^2)$]. Convergence to the final R values of $R = 0.0272$ and $R_w = 0.0282$ for **2b** was achieved by using 2944 reflections [$F^2 \geq 3\sigma(F^2)$]. Bond distances and angles, final positional and thermal parameters, observed and calculated structure factors, and crystallographic experimental details can be found in the supplementary material.
- Pearson, W. D. *Lattice Spacing and Structures of Metal and Alloys*; Pergamon: London, 1957.